Highly Crystalline Soluble Acene Crystal Arrays for Organic Transistors: Mechanism of Crystal Growth During Dip-Coating

Jaeyoung Jang, Sooji Nam, Kyuhyun Im, Jaehyun Hur, Seung Nam Cha, Jineun Kim, Hyung Bin Son, Hwansoo Suh, Marsha A. Loth, John E. Anthony, Jong-Jin Park, Chan Eon Park,* Jong Min Kim,* and Kinam Kim*

The preparation of uniform large-area highly crystalline organic semiconductor thin films that show outstanding carrier mobilities remains a challenge in the field of organic electronics, including organic field-effect transistors. Quantitative control over the drying speed during dip-coating permits optimization of the organic semiconductor film formation, although the kinetics of crystallization at the air–solution–substrate contact line are still not well understood. Here, we report the facile one-step growth of self-aligning, highly crystalline soluble acene crystal arrays that exhibit excellent field-effect mobilities (up to 1.5 cm V^{-1} s^{-1}) via an optimized dip-coating process. We discover that optimized acene crystals grew at a particular substrate lifting-rate in the presence of low boiling point solvents, such as dichloromethane (b.p. of 40.0 °C) or chloroform (b.p. of 60.4 °C). Variable-temperature dip-coating experiments using various solvents and lift rates are performed to elucidate the crystallization behavior. This bottom-up study of soluble acene crystal growth during dip-coating provides conditions under which one may obtain uniform organic semiconductor crystal arrays with high crystallinity and mobilities over large substrate areas, regardless of the substrate geometry (wafer substrates or cylinder-shaped substrates).

1. Introduction

Functionalized soluble acenes have recently attracted significant attention for use as active channel materials in organic field-effect transistors (OFETs) because of their strong solid-state intermolecular interactions and good intrinsic field-effect mobilities.[1–18] The solution processability of soluble acenes and their compatibility with rapid and easily controllable deposition methods offer a simple route to realizing low-cost flexible electronics.[1,3,7–9] The high performance of soluble acene-based OFETs can be achieved mainly by controlling the morphology and molecular packing of organic semiconductor molecules in the thin films during the self-organization process that occurs as the solvent evaporates.[10–18] In an effort to optimize the self-organization process, a variety of deposition methods have been used, such as drop-casting,[10–13,18] spin-coating,[13,14,17] and ink-jet printing.[15] Previous studies showed that slow solvent evaporation produced highly crystalline large grains in semiconductor thin-films, owing to sufficient time for self-organization among the organic semiconductor molecules.[10–18]

However, the preparation of highly crystalline uniform organic semiconductor thin films with high field-effect mobilities (exceeding 1.0 cm^2 V^{-1} s^{-1}) over a large substrate area still remains a challenge. Uniform soluble acene thin films may be obtained by spin-coating, but the films generally show low crystallinity because self-organization must occur within a remarkably short time (usually a few seconds).[18] Pre-modification of the interface[3] and post-annealing processes[17] have been used to increase the crystallinity. However, these processes complicate the fabrication process. Although slow evaporation approaches, such as drop-casting, produce highly ordered polycrystalline domains in which seed nucleation and evaporation-induced growth occurs, uniformity and reproducibility have not yet been achieved.[11,18] Recently, direct printing methods, such as ink-jet printing,[15] have provided precise deposition, yet this method may be inconsistent with reliable large-scale applications.

J. Jang, S. Nam, Dr. K. Im, Dr. J. Hur, Dr. S. N. Cha, Dr. J. Kim, Dr. H. B. Son, Dr. H. Suh, Dr. J.-J. Park, Prof. C. E. Park, Dr. J. M. Kim, Dr. K. Kim
Samsung Advanced Institute of Technology (SAIT)
Yongin, 449-712, Rep. Korea
E-mail: jongjin00.park@samsung.com; cep@postech.ac.kr; Jongkim@samsung.com

J. Jang, S. Nam, Prof. C. E. Park
Polymer Research Institute
Department of Chemical Engineering
Pohang University
of Science and Technology (POSTECH)
Pohang, 790-784, Rep. Korea

M. A. Loth, Prof. J. E. Anthony
Department of Chemistry
University of Kentucky
Lexington, Kentucky, 40506, USA

DOI: 10.1002/adfm.201102284

Coating techniques such as zone-casting, solution-shearing, and dip-coating can deposit uniaxially oriented organic semiconductor thin films that are desirable for OFETs due to the lower crystalline mismatch along the charge transport direction.[16,19–21] Processing optimization of these methods for improving the OFET performance has continuously been investigated. Because the drying speed can be quantitatively controlled during the dip-coating process by adjusting the substrate lifting rate, the method is suitable for depositing organic semiconductors and controlling their morphologies[22,23] Although a few studies have been directed toward understanding the self-organization mechanism of organic semiconductors with the goal of optimizing the processing conditions during dip-coating, the field-effect transistor performances have not been satisfactory (mobilities of <0.3 $cm^2 V^{-1} s^{-1}$).[16,22] Previous efforts manipulated the substrate lifting rate but did not consider cooperation among the solvent evaporation, capillary flow, and lifting rates. From this perspective, a systematic and in-depth study of the organic semiconductor solution crystallization kinetics at the air–solution–substrate contact line is necessary.

Here, we report the facile one-step growth of self-aligned, highly crystalline soluble acene crystal arrays that exhibit excellent field-effect mobilities (up to 1.5 $cm^2 V^{-1} s^{-1}$) via an optimized dip-coating process. In the dip-coating process, in contrast with slow evaporation approaches, low boiling point (b.p.) solvents (i.e., quickly evaporating solvents), such as dichloromethane or chloroform produce continuous and uniform crystals over large areas with high crystallinity. We further undertook experiments to elucidate the role of the solvent boiling point and substrate lifting rate on the crystal growth of soluble acenes during the dip-coating process. In particular, high-quality acene crystals were obtained on a substrate with a cylindrical fiber-shaped geometry as well as on wafer substrates, indicating that our method is versatile, useful, and potentially offers a foundation for demonstrating fiber-type organic-based electronic devices.

2. Results and Discussion

2.1. Characterization of the Acene Crystal Arrays

The organic semiconductors used in this study are 6,13-bis(tr iisopropylsilylethynyl) pentacene (TIPS-PEN) and fluorinated 5,11-bis(triethylsilylethynyl) anthradithiophene (FTES-ADT) (their chemical structures are shown in Figure S1 (Supporting Information)). They were dissolved in dichloromethane and chloroform, respectively, to form a 0.2 wt% solution. A substrate whose surface is 100 nm-thick Al_2O_3 layer was dipped into the solution and was lifted out at a constant rate of 10, 50, 100, 150, 200, or 300 μm/s. **Figures 1**a and 1b show polarized optical microscopy (POM) images of the dip-coated TIPS-PEN and FTES-ADT crystals formed from dichloromethane or chloroform, respectively. The acenes crystallized into continuous stripes in the upward lift direction at all rates slower than 300 μm/s (for dichloromethane) and 200 μm/s (for chloroform). At faster lifting rates, they dewetted by forming discontinuous islands as a result of inadequate time for continuous growth, which agreed with recent reports by Li et al.[22] As shown in the images (and plotted in Figure 1c), the average width and thickness of the crystals decreased with increasing lift rate. This trend is consistent with the data obtained from the θ–2θ mode out-of-plane X-ray diffraction (XRD) analysis shown in Figure S2 (Supporting Information). Thick crystals grown at 10 or 50 μm/s showed higher [00*l*] peak intensities than the crystals grown at faster lifting rates, for both acenes and solvents. In general, the intensity of the [00*l*] diffraction peaks is proportional not only to the crystallinity but also to the film thickness.[24,25] The diffraction patterns consisted of [00*l*] peaks with a *d* spacing of 16.6 Å (for TIPS-PEN) and 16.7 Å (for FTES-ADT), obtained from Bragg's law, $2d \sin\theta = n\lambda$. The *d* values for TIPS-PEN and FTES-ADT corresponded to their respective c-axis lengths, 16.83 Å and 16.65 Å.[5,6] Despite the large width and thickness of the slowly grown crystals (at 10 μm/s), crystals grown at a rate of 100 or 150 μm/s (for dichloromethane) and 50 μm/s (for chloroform) exhibited better uniformity in thickness (see Figure 1c) and consistent brightness and color in the POM images, suggesting better crystallinity.[26,27]

To obtain detailed information about the crystalline structure along the charge transport direction, we undertook high-resolution in-plane mode XRD analysis using a fixed grazing incidence angle of 0.15°, which lay suitably between the critical angle for total reflection by the acene crystals and the critical angle of the oxide insulator substrate (0.25°).[28] **Figures 2**a–d show, respectively, the in-plane XRD patterns of the TIPS-PEN and FTES-ADT crystals grown from dichloromethane and chloroform solvents, with the incident beam perpendicular to the crystal arrays, as illustrated in the inset of Figure 2a. The in-plane XRD pattern of the TIPS-PEN crystals contained only peaks corresponding to $d = 7.74$ Å, and the XRD pattern of FTES-ADT contained peaks corresponding to $d = 7.10$ Å, without other peaks, as in the case of the out-of-plane mode. This result indicated good crystallinity along the unit cell direction.[29,30] The *d* spacing matched the reported b-axis (7.75 Å for TIPS-PEN) and a-axis (7.10 Å for FTES-ADT) lengths, respectively.[5,6] The relative intensity of the first peaks for TIPS-PEN and FTES-ADT as a function of the substrate-lifting rate is plotted in Figures 2e and 2f, respectively. The crystals grown at 150 μm/s (for dichloromethane) and 50 μm/s (for chloroform) had the highest crystallinity in the in-plane direction for both acenes, as deduced from the POM images. This suggests the existence of an optimum lifting rate for promoting the crystallization of acenes, and that the solvent was critical for determining the optimum rate. The XRD studies showed that both TIPS-PEN and FTES-ADT crystallized in a triclinic unit cell, consistent with previous reports, and grew along the unit cell direction, as shown in Figures 2g and 2h, respectively.

To investigate the OFET characteristics of the crystals, top-contact OFETs were fabricated with Au source (S)/drain (D) electrodes, 100 nm-thick Al_2O_3 gate dielectric, and 200 nm-thick Al gate electrode. As shown in the inset images of **Figure 3** and Figure S3 (Supporting Information), individual crystals were characterized separately to accurately determine the crystal field-effect mobility (μ). Figures 3a and b show typical drain current (I_D) versus gate voltage (V_G) transfer characteristics, $I_D^{1/2}$ versus V_G characteristics for TIPS-PEN and FTES-ADT crystals grown with dichloromethane at different lifting rates, respectively. (Figure S3 (Supporting Information) shows those for TIPS-PEN and FTES-ADT crystals grown with a chloroform solvent at all

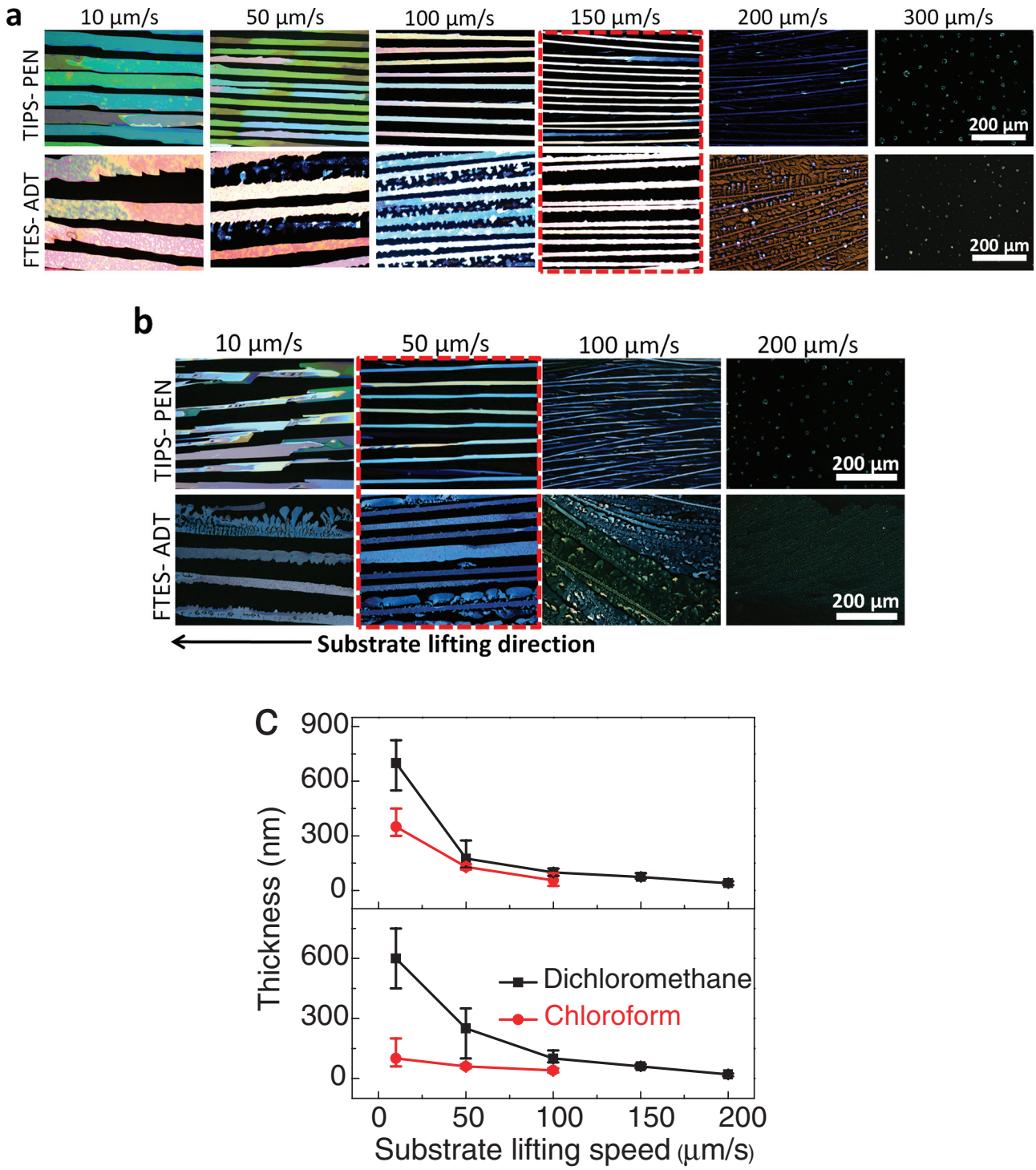

Figure 1. POM images of dip-coated TIPS-PEN (top) and FTES-ADT (bottom) crystals prepared from dichloromethane (a) and chloroform (b). The red rectangular borders indicate the optimal conditions. (c) The mean thickness of TIPS-PEN and FTES-ADT crystals from dichloromethane and chloroform solvents, plotted against the substrate lift rate.

lifting rates). **Table 1** summarizes the OFET characteristics of TIPS-PEN and FTES-ADT crystals grown at different lift rates from both solvents. As plotted in **Figures 4**a and b, the mobility values increased gradually as the lifting rate increased from 10 μm/s to 150 μm/s (for dichloromethane) and 50 μm/s (for chloroform). However, above those rates, the mobility eventually decreased. This trend in electrical characteristics is exactly consistent with the in-plane crystallinity and the morphological uniformity (from the POM images and thickness measurement) of the crystals with respect to the substrate-lifting rate. As

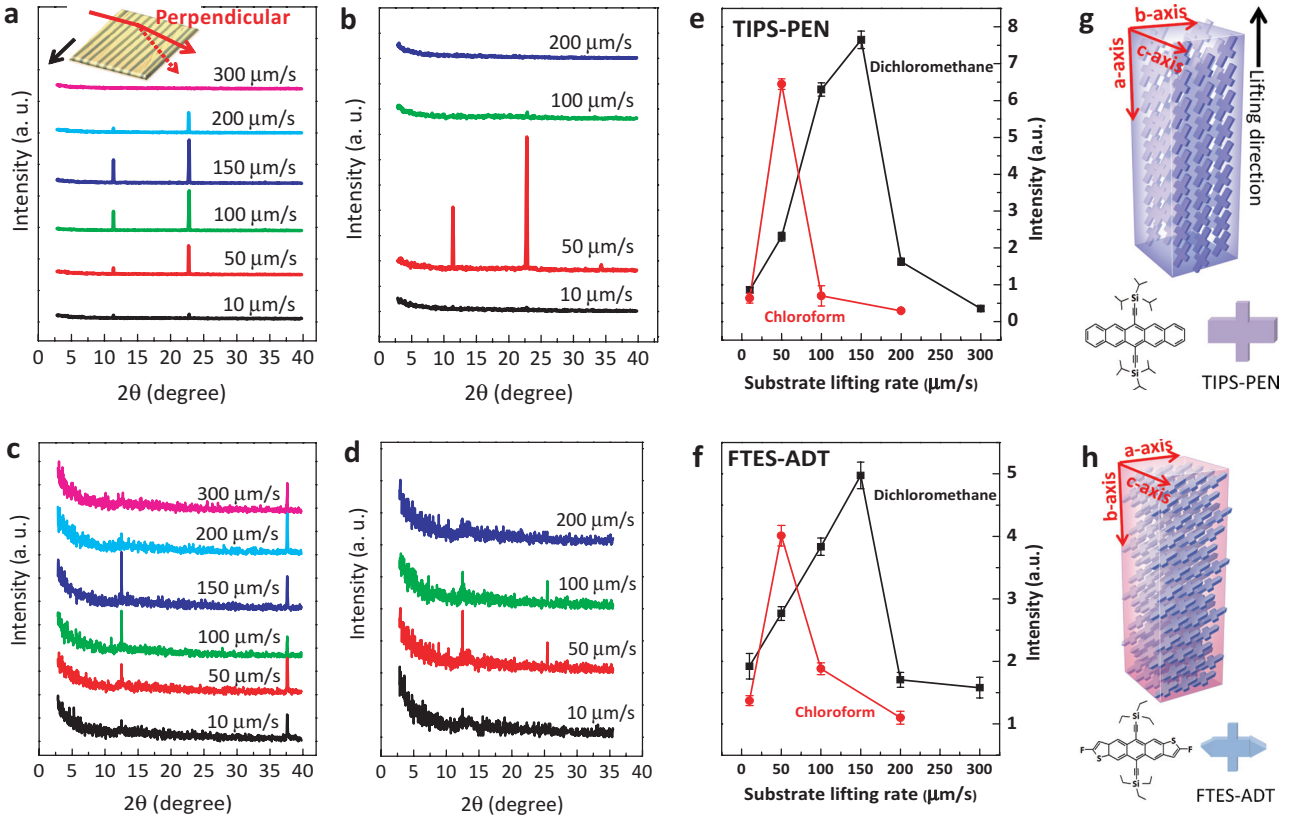

Figure 2. High-resolution grazing incidence (in-plane) XRD patterns for a) TIPS-PEN prepared from dichloromethane, b) TIPS-PEN prepared from chloroform, c) FTES-ADT prepared from dichloromethane, and d) FTES-ADT prepared from chloroform. The inset in (a) shows the incidence beam direction perpendicular to the crystal array. Relative intensities of the first peaks for e) TIPS-PEN and f) FTES-ADT crystals as a function of the substrate-lifting rate from both solvents. Schematic illustrations of crystal growth for g) TIPS-PEN and h) FTES-ADT showing their unit cell directions.

expected, the optimally crystallized TIPS-PEN and FTES-ADT (lifted at 150 μm/s from dichloromethane and at 50 μm/s from chloroform) exhibited superior field-effect mobilities which is orders of magnitude greater than those measured in crystals with different lifting rates. These crystals also show good I_D versus drain voltage (V_D) output characteristics as shown in Figures 4c and 4d. The POM, XRD, and electrical analyses presented above demonstrated that the optimum growth rates of soluble acene crystals, produced via dip-coating, were 150 μm/s for dichloromethane and 50 μm/s for chloroform.

A representative photograph, POM, and an atomic force microscopy (AFM) image of the optimally grown TIPS-PEN crystals (in dichloromethane at 150 μm/s) on a 2 cm × 5 cm wafer substrate were shown in Figure S4 (Supporting Information). As shown in those images and Figure S5 (Supporting Information), dozens of millimeters-long acene crystals covered the entire substrate area dipped in solution. Note that both acene crystals were reproducibly achieved over the entire dipped area of the substrate, regardless of the substrate size. Although the crystal alignment is somewhat irregular in the vicinity of the initial contact line, it becomes regular as the coating proceeds. We checked the uniformity of the optimally grown TIPS-PEN crystals. As illustrated in **Figure 5**a (also shown in Figure S4d (Supporting Information)), the non-contact mode AFM topograph and height profile indicated a uniform thickness of 95 ± 10 nm and an interval of 10 μm for three adjacent crystals. A POM image of a typical FET batch for the optimally grown TIPS-PEN crystals is shown in Figure S6 (Supporting Information). The average value and standard deviation of the effective channel width (the electrode width covering the crystals along the alignment direction) were found to be 19.54 and 2.87 μm, respectively. Arbitrarily selected 6–8 devices among them showed uniform field-effect mobilities (0.82–1.2 $cm^2\ V^{-1}\ S^{-1}$) and on-state currents.

We speculate that the regularity in initial nucleation sites of the dip-coated soluble acenes results from the fingering instability of the air–solution–substrate contact line.[31–33] In other words, when the substrate is pulled, the continuous line of soluble acenes at the air-solution-substrate contact line segregates into more concentrated, periodically distributed domains of soluble acenes due to the fingering instability of the drying front.[31–33] The regularly nucleated soluble acenes crystallized into continuous stripes as dip-coating proceeds, resulting in well-ordered crystal arrays.

2.2. Discussion of the Crystallization Behavior

The strong similarities in the crystallization behavior of TIPS-PEN and FTES-ADT dissolved in identical solvents suggest that the solvent plays an important role in the self-organization

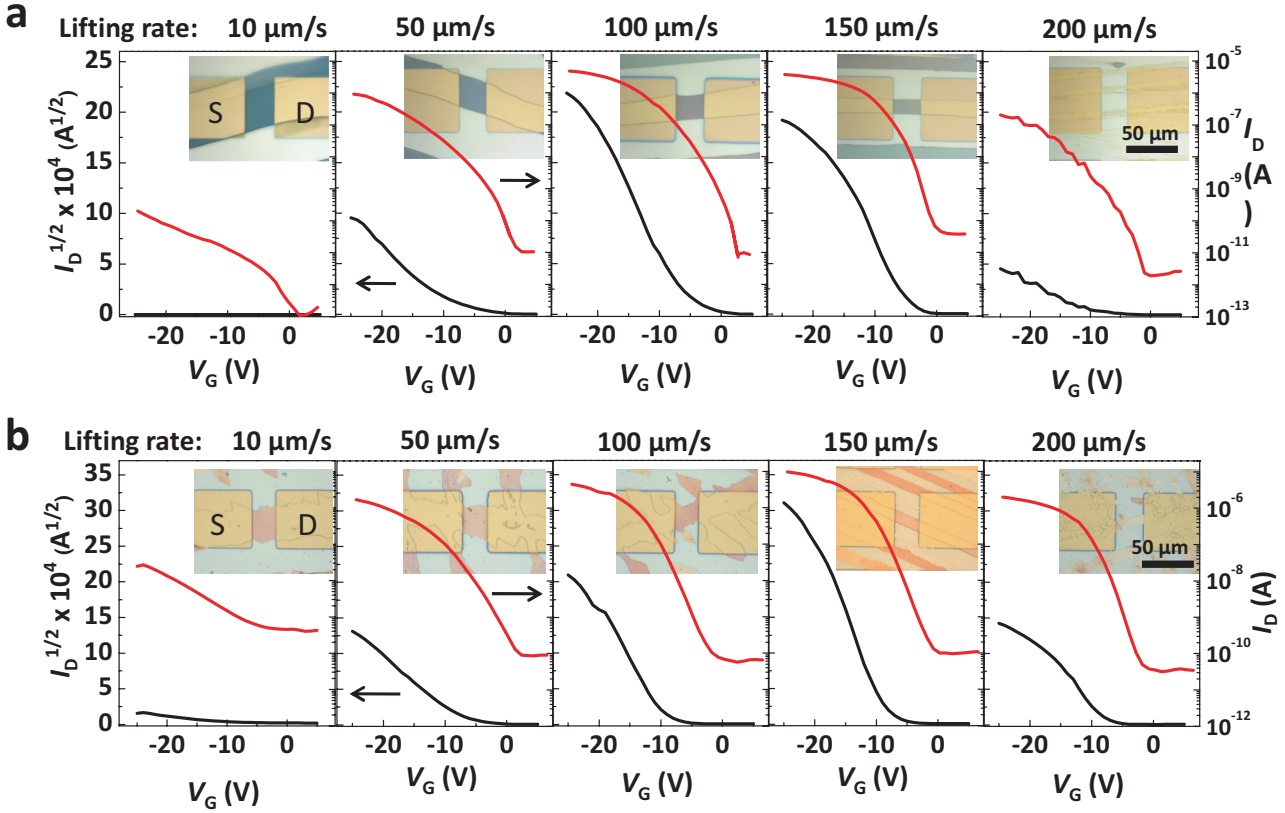

Figure 3. Typical I_D versus V_G transfer characteristics and $I_D^{1/2}$ versus V_G characteristics for a) TIPS-PEN and b) FTES-ADT crystals produced from dichloromethane as a function of the lift rates. The inset images show the individual crystal OFETs with Au source/drain electrodes. The scale bar indicates 50 μm.

Table 1. OFET characteristics of TIPS-PEN and FTES-ADT crystals prepared from dichloromethane and chloroform, grown at various substrate lift rates. A total of 24–40 FETs (6–8 FETs in a batch, 4–5 batches in total) were tested, and their OFET parameters were averaged for each experimental condition.

	Solvent	Device characteristics	Dip-coating rate (μm/s)					
			10	50	100	150	200	300
TIPS-PEN	dichloro-methane	μ (cm^2/Vs)	0.005	0.13	0.6–1.0	0.85–1.3	0.05	-
		On/off ratio	48	8.53×10^4	1.6×10^6	7.6×10^5	4.0×10^4	-
		V_{th} (V)	–7.4	–8.01	–7.63	–10.6	–10.2	-
		SS (V/dec)	6.4	1.89	1.66	1.3	1.54	-
TIPS-PEN	chloroform	μ (cm^2/Vs)	0.379	0.75 ~ 1.5	0.274	-	-	-
		On/off ratio	1.86×10^6	9.3×10^5	4.25×10^5	-	-	-
		V_{th} (V)	–7.95	–8.9	–5.76	-	-	-
		SS (V/dec)	1.75	2.1	1.64	-	-	-
FTES-ADT	dichloro-methane	μ (cm^2/Vs)	0.0013	0.05–0.3	0.1–0.9	0.92–1.5	0.1–0.3	-
		On/off ratio	73	1.2×10^5	4.02×10^5	1.0×10^5	2.7×10^5	-
		V_{th} (V)	–10.3	–7	–7.34	–8.6	–7.8	-
		SS (V/dec)	8.63	3.3	3.03	2.4	2.03	-
FTES-ADT	chloroform	μ (cm^2/Vs)	0.005	0.2–0.5	0.001	-	-	-
		On/off ratio	1.24×10^3	4.35×10^4	86	-	-	-
		V_{th} (V)	–8.6	–6.3	–6.7	-	-	-
		SS (V/dec)	3.6	2.1	3.2	-	-	-

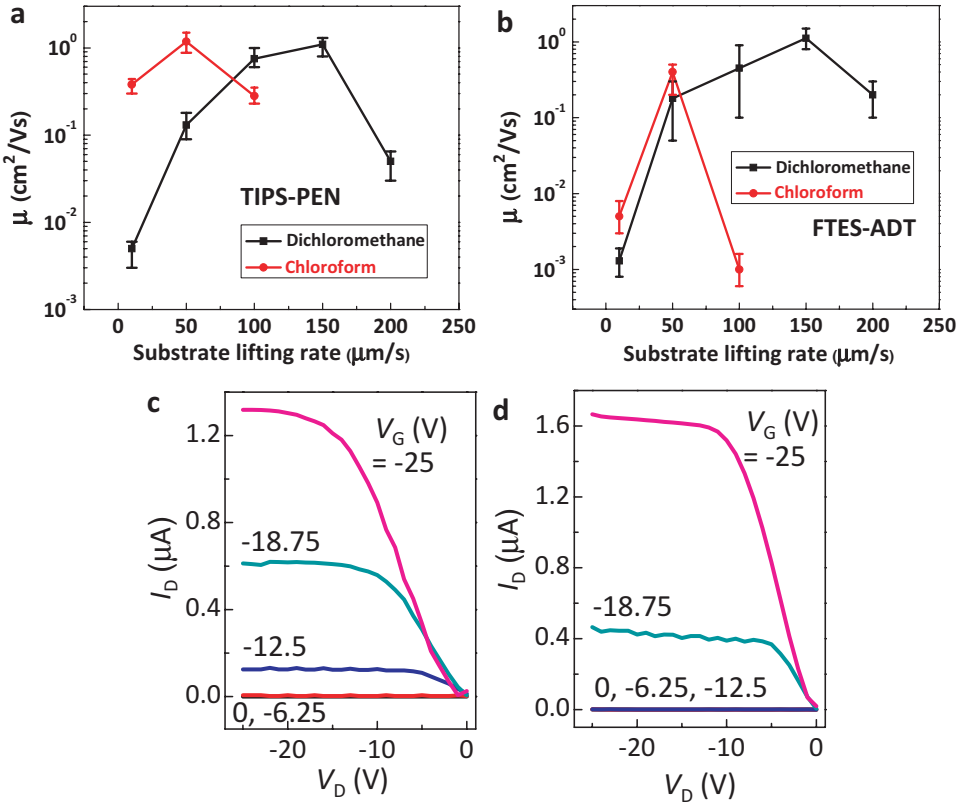

Figure 4. The μ values of a) TIPS-PEN and b) FTES-ADT crystals as a function of the substrate-lifting rate from dichloromethane and chloroform solvents. Typical I_D versus V_D output characteristics for c) TIPS-PEN and d) FTES-ADT crystals produced from dichloromethane solvent at a lifting rate of 150 μm/s.

process during dip-coating. Crystallization of organic semiconductors during dip-coating is an evaporation-induced process that occurs at the contact line.[16,22,34] When the contact line is strongly pinned, it experiences a "slip–stick" motion as a result of competition between the strong pinning force and the gradually increasing depinning force.[23,34–36] In this case, the semiconductor crystallized only when the contact line was confined to the substrate, and it failed to induce crystallization during the 'slip' state, resulting in regular patterns along the lift direction.[23,34] For our system, however, dozens of millimeters-long acene crystals covered the entire substrate length dipped in solution without producing empty regions along the lift direction (see Figures S4 and S5, Supporting Information). Also, the contact line is not pinned and the shape of the meniscus profile does not change at all until the dip-coating process had ended (see Figure S7, Supporting Information). These results strongly suggest that the growth rate of the crystals in our system was determined by the substrate lift rate. Furthermore, to maintain a steady state at the contact line, the rate of input and output flows (respectively, the evaporation-induced capillary flow toward the contact line and solvent evaporation at the contact line) should match the substrate lift rate, as illustrated in Figure 5b. To verify this relationship, we dip-coated TIPS-PEN using toluene as a solvent for comparison. The solubility parameter and surface tension of toluene were similar to those of dichloromethane and chloroform, but the b.p. of toluene (110.6 °C) was much higher that of dichloromethane or chloroform, as summarized in **Table 2**.[37] With toluene, TIPS-PEN crystallized discontinuously by producing empty regions at a lift rate of 10 μm/s due to the 'slip-stick' motion of the contact line. TIPS-PEN barely crystallized at lifting rates faster than 10 μm/s (Figure S8 (Supporting Information)). This phenomenon could be explained by the higher b.p. and the associated lower evaporation rate of toluene at the contact line. The slow evaporation rate did not keep up with the substrate lifting rate, so that TIPS-PEN crystallized in a discontinuous fashion with a 'slip-stick' contact line motion at 10 μm/s. It minimally crystallized at faster substrate lifting rates as well. These results suggest that the fast evaporation rate of dichloromethane and chloroform at the contact line improved the growth of highly crystalline continuous acene crystals during the dip-coating process. In fact, some reports have described dip-coated TIPS-PEN OFETs using toluene as the solvent, but their μ values were an order of magnitude lower than those of our OFETs, which used a fast evaporation system, and similar to the mobilities of our OFETs prepared from toluene. (see Table S1, Supporting Information).[16,38]

Why should the substrate lifting rate display an optimal value for crystallization and growth of acenes, and why does it depend on the solvent used, dichloromethane or chloroform? In our system, the crystal growth rate at the contact line along the lift direction was determined by the substrate lifting rate. The

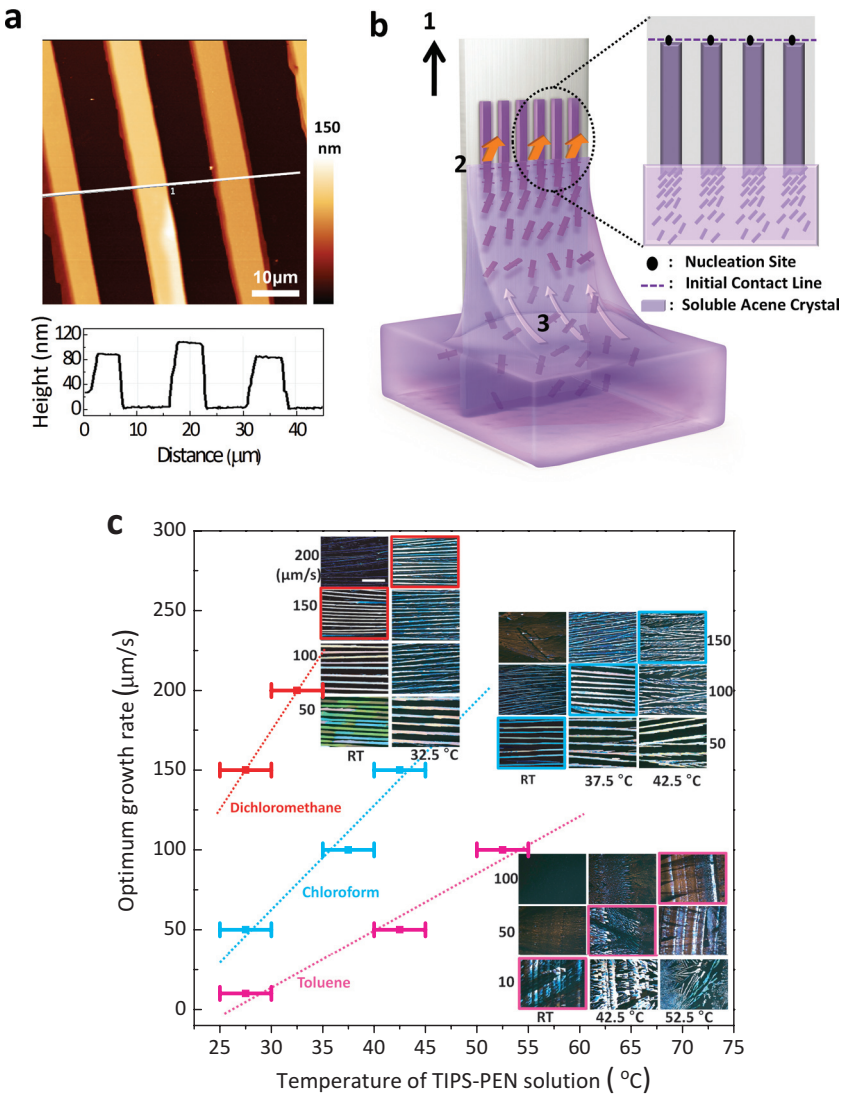

Figure 5. a) An AFM image of the optimally grown TIPS-PEN crystals (in dichloromethane at 150 μm/s) (top) and a height profile of the three adjacent crystals (bottom). b) Simplified schematic illustration of fast evaporation-induced crystal growth, and magnification of the contact line. c) Temperature dependence of the optimum growth rate of TIPS-PEN for the various solvents. The insets show POM images of the TIPS-PEN crystals that correspond to each experimental condition. Here, the optimum growth rate is the substrate lift rate that produces crystals with highest OFET mobilities. Colored rectangular borders represent the optimal conditions. The scale bar indicates 200 μm.

acene molecules were over-stacked at lifting rates lower than the optimal rate because the contact line remained at the substrate for a longer time. It is difficult for excess acene molecules to crystallize uniformly with directional growth, which produces large concentrations of grain boundaries in thick crystals with poor in-plane crystallinity.[24,39] Conversely, when the lifting rate exceeds the optimum rate, the acenes do not have sufficient time to crystallize directionally, and they dewet. Therefore, we can speculate that the optimum condition is the condition where the substrate lift rate and the rate of input/output at the contact line are the most well-balanced for the directional growth of the acene crystals, under a given acene material. Obviously, the optimal substrate lift rate may depend on the crystallization tendency of the acene itself. For example, we also tried to dip-coat another soluble acene derivative, 5,11-bis(triethylsilylethynyl) anthradithiophene (TES-ADT), whose crystallization tendency is very weak (therefore, post solvent anealing processes are essentially required to improve the film crystallinity).[8,17] As a result, the optimal substrate lift rate for the TES-ADT with dichloromethane solvent is found to be 10 μm/s (data not shown). Note also that the optimal characteristics of the acene crystals (TIPS-PEN and FTES-ADT) were similar in chloroform and dichloromethane, although the optimum growth rates for the solvents were different. These results may suggest the following: (1) the optimal mechanisms for crystallization and growth of the soluble acenes during dip-coating were probably similar in chloroform and dichloromethane solvents, even though the solvent boiling point significantly influences the solution crystallization kinetics, and (2) the lower optimum growth rate for chloroform (50 μm/s) than for dichloromethane (150 μm/s) was likely due to the higher b.p. and lower evaporation rate of chloroform compared with dichloromethane.

To gain further insight, we studied the temperature-dependence of the optimum growth rate for various solvents. We repeatedly dip-coated TIPS-PEN in dichloromethane (at RT (27.5 °C) and at 32.5 °C), in chloroform (at RT, 37.5 °C, and 42.5 °C), and in toluene (at RT, 42.5 °C, and 52.5 °C). Figure 5c shows a plot of the optimum growth rate of TIPS-PEN crystals as a function of solution temperature for dichloromethane, chloroform, and toluene, and the inset shows POM images of the resulting crystals (the corresponding OFET characteristics and overall POM images of the resulting crystals are summarized and shown in Table S1 and Figure S9 in the Supporting Information, respectively). The solution, in a glass vial, was placed on a hot plate with a controlled temperature, and dip-coating was carried out in batches with substrate lifting rates ranging from 10 to 300 μm/s. Solvent evaporation at the contact line and evaporation-induced capillary flow toward

Table 2. Summary of the various solvent parameters for dichloromethane, chloroform, and toluene.

	Boiling point (°C)	Solubility parameter [(cal/cm^3)$^{1/2}$]	Surface tension at 25 °C (dyn/cm)	Concentration of acenes (w.t.%)
dichloromethane	40.0	9.7	26.52	0.2
chloroform	60.4	9.3	27.1	0.2
toluene	110.6	8.9	28.52	0.2

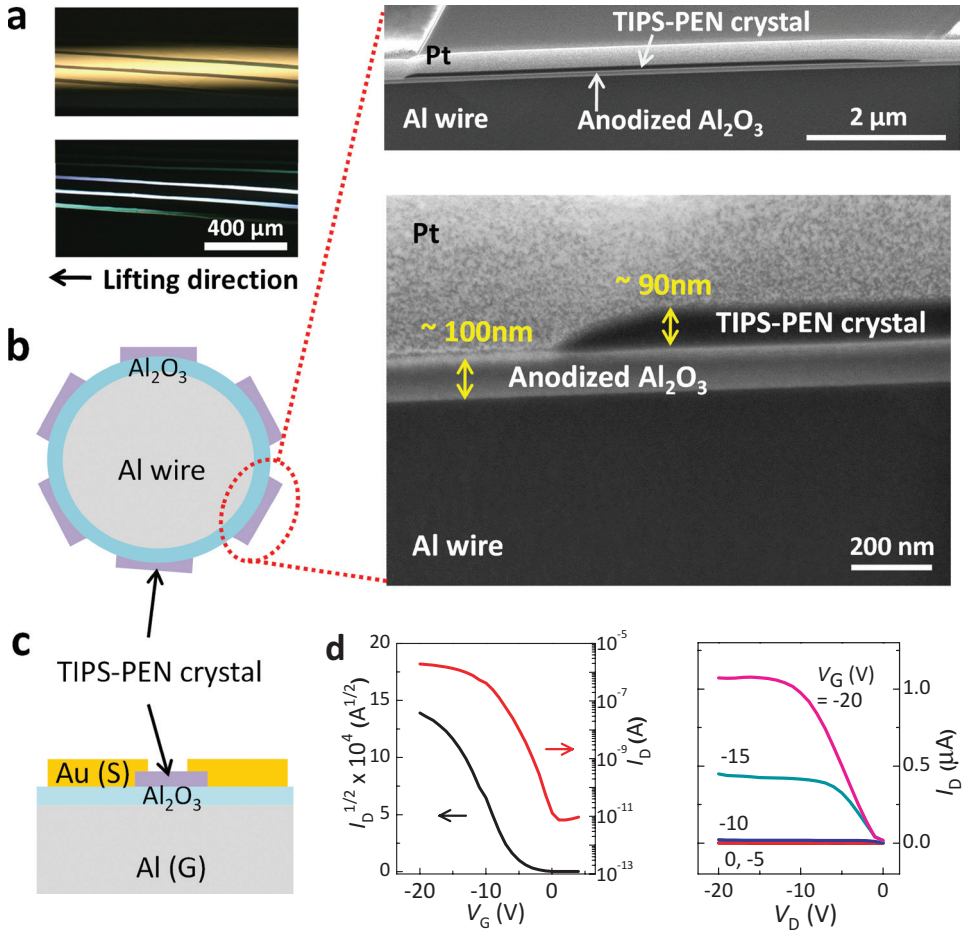

Figure 6. a) OM and POM images of optimally grown (at 150 µm/s from dichloromethane) TIPS-PEN crystals on an Al wire. b) A schematic cross-section of the TIPS-PEN crystal grown on an Al wire (left), a cross-sectional SEM image of the TIPS-PEN crystal milled by FIB grown on an Al wire (top), and a magnified SEM image (bottom). c) A schematic device cross-section. (d) Typical transfer and output characteristics for TIPS-PEN from dichloromethane at a lifting rate of 150 µm/s

the contact line were expected to increase as the solution is heated.[40,41] As a result, the optimum growth rate increased as the temperature was raised, where the optimum growth rate indicated the substrate lifting rate that produced crystals with the highest OFET mobility. These results imply that optimum crystals may be achieved for substrate lifting rates that are the most well-balanced with the solvent evaporation and evaporation-induced capillary flow at the chosen solution temperature. This study clearly showed that optimal acene crystals could be obtained when the rate of input/output flows at the contact line is well-balanced with the substrate lifting rate. Accordingly, fast-evaporating solvents, such as dichloromethane or chloroform, were appropriate for the crystal growth of the soluble acenes during the dip-coating process.

2.3. Formation of the Crystal Array on a Cylindrical Substrate

To guarantee the versatility and utility of our work and to confirm the optimal crystal growth behavior, we dip-coated TIPS-PEN on a substrate with a non-flat geometry, a cylindrical fiber-shaped Al wire. Prior to dip-coating, the Al wire was anodized to form a 100 nm thick Al_2O_3 gate dielectric (**Figure 6**b).[42] The TIPS-PEN crystals formed during dip-coating with dichloromethane or chloroform on the Al wire substrates showed morphological trends with respect to the substrate lifting rates that were similar to those of crystals grown on flat wafers (the optimal growth rate for dichloromethane: 150 µm/s and for chloroform: 50 µm/s, see their corresponding POM images in Figure S10, Supporting Information). We further investigated the TIPS-PEN crystal arrays optimally grown from dichloromethane on an Al wire. Figure 6a shows OM and POM images of the crystals, and Figure 6b shows tilted view scanning electron microscopy (SEM) images of a cross-section taken after focused ion beam (FIB) milling of the TIPS-PEN crystal. A thickness of 90 nm was consistent with the average thickness of the optimally grown crystals on flat wafers. Finally, OFET characteristics of the crystals were obtained by fabricating top-contact OFETs. As in the case of the crystals grown on flat wafers, 1 or 2 crystals were characterized separately to allow accurate measurement of the crystal field-effect mobility (see the schematic device cross-section and top-view images of the devices in Figure S10, Supporting Information). The TIPS-PEN crystals optimally grown on an Al wire also exhibited superior field-effect mobilities of

0.65–1.1 $cm^2 V^{-1} s^{-1}$ with good I_D versus V_D output characteristics, including clear linear and saturation regions (see their transfer and output curves in Figure S10, Supporting Information). These results strongly support our conclusion, and further suggest that the proper banalnce among the rate of input/output flows at the contact line and the substrate lifting rate is more crucial than the other experimental conditions for determining the optimum growth rate of soluble acene crystal arrays during the dip-coating process. Because dip-coating is not significantly influenced by the geometry of the substrate, unlike other coating methods (i.e., spin-coating, drop-casting, or direct printings), our facile one-step growth of soluble acene crystal arrays has great potential for preparing unconventional devices, such as cylinder-shaped fiber-type electronic devices for use in wearable electronics.[43,44]

3. Conclusions

In conclusion, we have demonstrated the facile one-step growth of highly crystalline uniform soluble acene crystal arrays with outstanding OFET mobilities (up to 1.5 $cm^2 V^{-1}s^{-1}$) over large areas via an optimized dip-coating method using quickly evaporating solvents. To improve our understanding of the relationship among the solvent evaporation rate, the substrate lifting rate, and the crystal growth, we systematically manipulated the solvent evaporation rate and substrate lifting rate during dip-coating of the soluble acenes. We showed that optimized crystals were grown when the rate of input/output flows at the contact line is well-balanced with the substrate lifting rate. This conclusion was supported by optical, crystallographic, morphological, and electrical analysis of the acene crystals, as well as by variable-temperature dip-coating experiments with various solvents and lifting rates. The results of our study elucidate the organic semiconductor solution crystallization kinetics at the air–solution–substrate contact line. As a result, we suggest a simple and reproducible method for creating high-performance uniform organic semiconductor thin films over large areas of substrates with a variety of geometries (wafer substrates or cylinder-shaped substrates).

4. Experimental Section

Materials and Sample Preparation: For OFET devices fabrication, heavily doped n-type Si wafers with a 200 nm thick Al gate were used as substrates. An Al_2O_3 gate dielectric layer, 100 nm thick, was deposited on the substrate by atomic layer deposition (ALD). The substrate was dipped into a TIPS-PEN (assay ≥99, Aldrich) or FTES-ADT (as synthesized by Anthony and co-workers)[6] solution (0.2 wt% in dichloromethane, chloroform, or toluene) at a constant rate of 1000 μm/s, and was then lifted out at a constant rate of 10, 50, 100, 150, 200, or 300 μm/s. Dip-coating was performed in an acrylic box on a shock-absorbing optical table for reducing the effect of air currents, mechanical vibration, and noise. Gold S/D electrodes were formed by thermal evaporation using a shadow mask on the active layer. Each of the resulting square gold patterns had a 55.0 μm width, and the interval between patterns was 22.5 μm, as shown in the inset of Figures 3 and S3. The channel length (L) and width (W) of each transistor were determined from optical micrographs. OFETs were fabricated on Al wire substrates by anodizing an Al wire (Aldrich, diameter was measured by 700 μm with a caliper) at a constant current density of 0.32 mA/cm^2 at 80 V in 0.05 M ammonium pentaborate octahydrate electrolyte at 25 °C so as to form a 100 nm thick Al_2O_3 gate dielectric layer around the Al wire.[42] The wire substrate was dipped into a TIPS-PEN solution (0.2 wt% in dichloromethane or chloroform) at a constant rate of 1000 μm/s, then lifted out at a constant rate of 10, 50, 100, 150, 200, or 300 μm/s. The field-effect mobility of each crystal formed on the wire was measured according to the method used for measuring OFET performance of crystals grown on the flat wafer substrates.

Characterization: The thickness of the acene crystals was determined using a surface profiler (Alpha-step 500, KLA Tencor). The OM and POM images were obtained using an optical microscope (OLS 3000, Olympus). All POM images were recorded under cross polarization with same polarizer angle. High-resolution out-of-plane and grazing incidence in-plane XRD experiments were performed at the 10C1 beamline (λ = 1.54 Å) at the Pohang Accelerator Laboratory, Pohang, Korea. AFM images were collected using an atomic force microscope (XE, Park Systems). SEM images were obtained using a field-emission scanning electron microscope (S-4800, Hitachi). The TIPS-PEN crystals were machined using a dual beam FIB instrument (FIB2200, Seiko). The conditions for milling were 30 kV for the I-beam. Side view images were collected with a typical positive slope of 52°. All *I-V* characteristics of the devices and capacitances per unit area (C_i) of the gate dielectrics were measured in ambient air (relative humidity, 45 ± 15%) using a source/measurement unit (Keithley 4200) and a 4284 precision LCR meter (Agilent Tech), respectively. The mean C_i values for the 100 nm thick Al_2O_3 gate dielectrics on wafer (deposited by ALD) and wire (deposited by anodization) substrates were found to be, respectively, 64 nF/cm^2 and 58 nF/cm^2. The field-effect mobility of each acene crystal was calculated from the transfer curves in the saturation regime, swept over the V_G range +5 to–25 V for OFETs on the Al wafer substrates, and +5 to–20 V for OFETs on the Al wire substrates, using the equation, $I_D = \mu C_i W(2L)^{-1}(V_G - V_{th})^2$ where V_{th} is the threshold voltage. A total of 24–40 FETs (6–8 FETs in a batch, 4–5 batches in total) were tested, and their FET parameters were averaged for each experimental condition (acene material, solvent, and substrate lift rate).

Supporting Information

Supporting Information is available from the Wiley Online Library or from the author.

Acknowledgements

J.J. and S.N. contributed equally to this work. This work was supported by a grant from the Korea Science and Engineering Foundation (KOSEF) and National Research Foundation of Korea as a part of Global Frontier Research Center for Advanced Soft Electronics, funded by the Korea government (MEST) (20110000330).

Received: September 25, 2011
Revised: October 28, 2011
Published online: January 18, 2012

[1] G. H. Gelinck, H. E. A. Huitema, E. V. Veenendaal, E. Canatatore, L. Schrijnemakers, J. B. P. H. V. D. Putten, T. C. T. Geuns, M. Beenhakkers, J. B. Giesbers, B.-H. Huisman, E. J. Meijer, E. M. Benito, F. J. Touwslager, A. W. Marsman, B. J. E. V. Rens, D. M. D. Leeuw, *Nat. Mater.* **2004**, *3*, 106.
[2] J. E. Anthony, *Angew. Chem. Int. Ed.* **2008**, *47*, 452.
[3] D. J. Gundlach J. E. Royer, S. K. Park, S. Subramanian, O. D. Jurchescu, B. H. Hamadani, A. J. Moad, R. J. Kline, L. C. Teague, O. Kirillov, C. A. Richter, J. G. Kushmerick, L. J. Richter, S. R. Parkin, T. N. Jackson, J. E. Anthony, *Nat. Mater.* **2008**, *7*, 216.
[4] D. S. Chung, J. W. Park, J.-H. Park, D. Moon, G. H. Kim, H.-S. Lee, D. H. Lee, H.-K. Shim, S.-K. Kwon, C. E. Park, *J. Mater. Chem.* **2010**, *20*, 524.

[5] J. E. Anthony, J. S. Brooks, D. L. Eaton, S. R. Parkin, *J. Am. Chem. Soc.* **2001**, *123*, 9482.
[6] S. Subramanian, S. K. Park, S. R. Parkin, V. Podzorov, T. N. Jackson, J. E. Anthony, *J. Am. Chem. Soc.* **2008**, *130*, 2706.
[7] S. J. Kang, Y. J. Park, I. Bae, K. J. Kim, H.-C. Kim, S. Bauer, E. L. Thomas, C. Park, *Adv. Funct. Mater.* **2009**, *19*, 2812.
[8] W. H. Lee, J. A. Lim, D. Kwak, J. H. Cho, H. S. Lee, H. H. Choi, K. Cho, *Adv. Mater.* **2009**, *21*, 4243.
[9] D. S. Chung, W. M. Yun, S. Nam, S. H. Kim, C. E. Park, J. W. Park, S.-K. Kwon, Y.-H. Kim, *Appl. Phys. Lett.* **2009**, *94*, 043303.
[10] C. S. Kim, S. Lee, E. D. Gomez, J. E. Anthony, *Appl. Phys. Lett.* **2008**, *93*, 103302.
[11] Z. He, K. Xiao, W. Durant, D. K. Hensley, J. E. Anthony, K. Hong, S. M. Kilbey II, J. Chen, D. Li, *Adv. Funct. Mater.* **2011**, *21*, 3617.
[12] S. H. Kim, D. Choi, D. S. Chung, C. Yang, J. Jang, C. E. Park, S.-H. K. Park, *Appl. Phys. Lett.* **2008**, *93*, 113306.
[13] S. K. Park, T. N. Jackson, J. E. Anthony, D. A. Mourney, *Appl. Phys. Lett.* **2007**, *91*, 063514.
[14] Y.-H. Kim, Y. U. Lee, J.-I. Han, S.-M. Han, M.-K. Han, *J. Electrochem. Soc.* **2007**, *154*, H995.
[15] J. A. Lim, W. H. Lee, H. S. Lee, J. H. Lee, Y. D. Park, K. Cho, *Adv. Funct. Mater.* **2008**, *18*, 229.
[16] C. W. Sele, B. K. C. Kjellander, B. Niesen, M. J. Thornton, J. B. P. H. van der Putten, K. Myny, H. J. Wondergem, A. Moser, R. Resel, A. J. J. M. van Breemen, N. van Aerle, P. Heremans, J. E. Anthony, G. H. Gelinck, *Adv. Mater.* **2009**, *21*, 4926.
[17] K. C. Dickey, J. E. Anthony, Y.-L. Loo, *Adv. Mater.* **2006**, *18*, 1721.
[18] J. H. Park, K. H. Lee, S.-j. Mun, G. Ko, S. J. Heo, J. H. Kim, E. Kim, S. Im, *Org. Electron.* **2010**, *11*, 1688.
[19] W. Pisula, A. Menon, M. Stepputat, I. Lieberwirth, U. Kolb, A. Tracz, H. Sirringhaus, T. Pakula, K. Müllen, *Adv. Mater.* **2005**, *17*, 684.
[20] H. A. Becerril, M. E. Roberts, Z. Liu, J. Locklin, Z. Bao, *Adv. Mater.* **2008**, *20*, 2588.
[21] C. M. Duffy, J. W. Andreasen, D. W. Breiby, M. M. Nielsen, M. Ando, T. Minakata, H. Sirringhaus, *Chem. Mater.* **2008**, *20*, 7252.
[22] L. Li, K. C. Schuermann, S. Ostendorp, W. Wang, C. Du, Y. Lei, H. Fuchs, L. de Cola, K. Müllen, L. Chi, *J. Am. Chem. Soc.* **2010**, *132*, 8807.
[23] J. Huang, R. Fan, S. Connor, P. Yang, *Angew. Chem. Int. Ed.* **2007**, *46*, 2414.
[24] H.-L. Cheng, Y.-S. Mai, W.-Y. Chou, L.-R. Chang, X.-W. Liang, *Adv. Func. Mater.* **2007**, *17*, 3639.
[25] D. J. Gundlach, Y. Y. Lin, T. N. Jackson, S. F. Nelson, D. G. Schlom, *IEEE Electron Device Letters* **1997**, *18*, 87.
[26] H. A. Becerril, M. E. Roberts, Z. Liu, J. Locklin, Z. Bao, *Adv. Mater.* **2008**, *20*, 2588.
[27] J. Rivnay, L. H. Jimison, J. E. Northrup, M. F. Toney, R. Noriega, S. Lu, T. J. Marks, A. Facchetti, A. Salleo, *Nat. Mater.* **2009**, *8*, 952.
[28] F. H. Fabreguette, R. A. Wind, S. M. George, *Appl. Phys. Lett.* **2006**, *88*, 013116.
[29] W. H Lee, D. H. Kim, Y. Jang, J. H Cho, M. Hwang, Y. D. Park, Y. H. Kim, J. I. Han, K. Cho, *Appl. Phys. Lett.* **2007**, *90*, 132106.
[30] O. D. Jurchescu, S. Subramanian, R. J. Kline, S. D. Hudson, J. E. Anthony, T. N. Jackson, D. J. Gundlach, *Chem. Mater.* **2008**, *20*, 6733.
[31] J. Huang, F. Kim, A. R. Tao, S. Connor, P. Yang, *Nat. Mater.* **2005**, *4*, 896.
[32] A. M. Cazabat, F. Heslot, S. M. Troian, P. Carles, *Nature* **1990**, *346*, 824.
[33] S. D. Fitzgerald, A. W. Woods, *Nature* **1994**, *367*, 450.
[34] C. Zhang, X. Zhang, X. Zhang, X. Fan, J. Jie, J. C. Chang, C.-S. Lee, W. Zhang, S.-T. Lee, *Adv. Mater.* **2008**, *20*, 1716.
[35] R. D. Deegan, O. Bakajin, T. F. Dupont, G. Huber, S. R. Nagel, T. A. Witten, *Nature* **1997**, *389*, 827.
[36] R. van Hameren, P. Schön, A. M. van Buul, J. Hoogboom, S. V. Lazarenko, J. W. Gerritsen, H. Engelkamp, P. C. M. Christianen, H. A Heus, J. C. Maan, T. Rasing, S. Speller, A. E. Rowan, J. A. A. W. Elemans, R. J. M. Nolte, *Science* **2006**, *314*, 1433.
[37] S. L. Rosen, in *Fundamental Principles of Polymeric Materials*, 2nd ed., John Wiley & Sons, New York **1993**.
[38] R. L. Headrick, S. Wo, F. Sansoz, J. E. Anthony, *Appl. Phys. Lett.* **2008**, *92*, 063302.
[39] S. Joshi, S. Grigorian, U. Pietsch, P. Pingel, A. Zen, D. Neher, U. Scherf, *Macromolecules* **2008**, *41*, 6800.
[40] E. Treossi, A. Liscio, X. Feng, V. Palermo, K. Müllen, P. Samorì, *Small* **2009**, *5*, 112.
[41] N. Liu, Y. Zhou, L. Wang, J. Peng, J. Wang, J. Pei, Y. Cao, *Langmuir* **2009**, *25*, 665.
[42] C. Yang, K. Shin, S. Y. Yang, H. Jeon, D. Choi, D. S. Chung, C. E. Park, *Appl. Phys. Lett.* **2006**, *89*, 153508.
[43] B. O'Connor, K. H. An, Y. Zhao, K. P. Pipe, M. Shtein, *Adv. Mater.* **2007**, *19*, 3897.
[44] M. Hamedi, L. Herlogsson, X. Crispin, R. Marcilla, M. Berggren, O. Inganäs, *Adv. Mater.* **2009**, *21*, 573.